Applied Physics Letters ARTICLE scitation.org/journal/apl

High transmittance Er-doped ZnO thin films as electrodes for organic light-emitting diodes

Cite as: Appl. Phys. Lett. **115**, 252102 (2019); doi: 10.1063/1.5129065
Submitted: 25 September 2019 · Accepted: 30 November 2019 ·
Published Online: 16 December 2019

Ying-Li Shi,[1,a)] Yun Hu,[2] Shuang-Peng Wang,[3] Liang-Sheng Liao,[2,a)] and Francis Chi-Chung Ling[1,a)]

AFFILIATIONS

[1]Department of Physics, The University of Hong Kong, Hong Kong 999077, People's Republic of China
[2]Jiangsu Key Laboratory for Carbon-Based Functional Materials & Devices, Institute of Functional Nano & Soft Materials (FUNSOM), and Collaborative Innovation Center of Suzhou Nano Science and Technology, Soochow University, Suzhou 215123, People's Republic of China
[3]Institute of Applied Physics and Materials Engineering, University of Macau, Macau 999078, People's Republic of China

[a)]**Authors to whom correspondence should be addressed:** ylshi@connect.hku.hk and ccling@hku.hk

ABSTRACT

Rare earth element-Erbium (Er) doped ZnO (ErZO) thin films were deposited on glass substrates by pulsed laser deposition (PLD). The effect of the Er doping concentration on photoelectric properties of ErZO thin films was investigated in the range of 0–2.0 wt. %. The Er doping resulted in the improvement of *n*-type conductivity as compared with intrinsic ZnO thin films. The optimized ErZO thin films present the low resistivity of 3.4×10^{-4} Ω/cm, high carrier concentration of 5.9×10^{20}/cm^3, and high visible optical transmittance (∼93%) when the Er content is 1.0 wt. %. The ErZO thin films were used as transparent anodes to fabricate organic light-emitting diodes (OLEDs). Impressively, with ErZO as the anode, the current efficiency of the OLED device can reach as high as 86.5 cd/A, which was increased by 14% when compared with the reference OLED device (76.0 cd/A) using indium tin oxide as the anode.

Transparent conducting oxides (TCOs) have attracted great attention since their first demonstration in 1907 by Baedeker.[1] TCO thin films with high transparency and electrical conductivity have been widely used in optoelectronic devices, such as thin-film transistors, perovskite solar cells, organic light-emitting diodes (OLEDs), and quantum dot light emitting diodes (QLEDs).[2–5] In the area of optoelectronic devices, transmittance and conductivity are two important factors that affect device performance.

Ga-doped and Al-doped ZnO is considered to be the promising TCO material to replace indium tin oxide (ITO) owing to its attractive properties, such as the wide bandgap (∼3.37 eV), high transmittance in the visible light (∼90%), being rich in raw materials, and compatibility with the environment.[6] Tremendous research has been performed to achieve high quality n^+-type ZnO based TCO thin films via substituting Zn with group III elements (such as Ga, Al, In, Ti, and Y) or replacing O with group VII elements (such as F, Cl, and Br).[7–10] Recently, Jaroslav Bruncko *et al.* deposited Ga-doped ZnO (GZO) thin films by pulsed laser deposition (PLD) and investigated the influence of deposition temperature and laser pulse frequency on GZO film properties.[8] Eventually, the optimized GZO film shows a low resistivity of 5.96×10^{-4} Ω/cm and a high carrier concentration of 14.6×10^{21}/cm^3. Cristian Ursu *et al.* obtained Al-doped ZnO (AZO) thin films through sequential PLD (SPLD) with high optical transmittance (∼90%) and a low resistivity of 5.1×10^{-4} Ω/cm.[9] With radio frequency magnetron sputtering, Pak *et al.* reported a Ga-doped ZnO film deposited on c-plane sapphire, which has an electron concentration and optical transmittance in the visible wavelength of 7×10^{20}/cm^3 and 94%.[10] In addition, Hyung-Ho Park *et al.* prepared F doped ZnO (FZO) thin films by atomic layer deposition (ALD). This FZO film also shows a low resistivity of 1.876×10^{-3} Ω/cm corresponding to a carrier density of 1.375×10^{20}/cm^3.[11]

The effect of rare earth ions as impurity dopants for ZnO on structural, optical, and electrical properties has been investigated in recent years.[12–17] Tadatsugu Minami *et al.* doped ZnO with rare-earth elements Sc and Y to fabricate ZnO based TCO thin films by magnetron sputtering.[16] The lowest resistivities of 3.1×10^{-4} Ω/cm and 7.9×10^{-4} Ω/cm were obtained in ZnO:Sc and ZnO:Y thin films, respectively, with the average transmittance of above 85%. Last year, Xingyuan Liu *et al.* reported the Eu and F co-doped ZnO (EFZO) thin film by ion-assisted electron beam evaporation.[17] The optimized EFZO film shows an average optical transmittance of 82.9% and a resistivity of 5.7×10^{-4} Ω/cm. The EFZO based organic and quantum

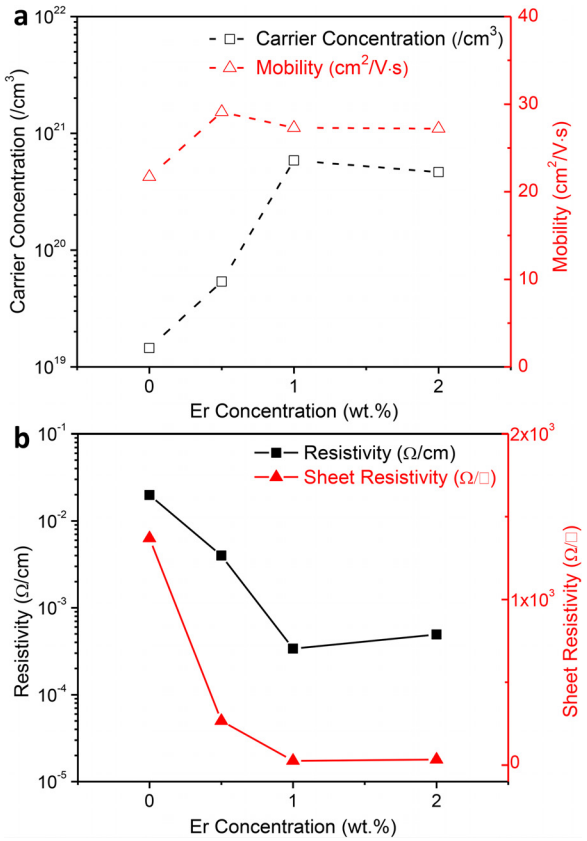

FIG. 1. Electrical properties of ErZO films measured by the Hall Effect system. (a) Carrier concentration and mobility as a function of Er concentration. (b) Resistivity and sheet resistivity as a function of Er concentration.

dot light-emitting diodes show equivalent or a little higher electroluminescence performance in comparison to the ITO-based devices.

Er-doped ZnO is a desired optoelectronic material because of its intra-4f transition related emission at 1.54 μm used in telecommunication technology for the maximum transmittance in SiO_2-based optical fiber. Moreover, Er-doped ZnO films exhibit higher optical transparency (~95%) than other reported metal element doped ZnO TCO thin films.[18–20] In this work, we deposited Er-doped ZnO TCO thin films on glass substrates and investigated the influence of the Er concentration on structural, optical, and electrical characteristics. It has been reported that the Er^{3+} substitution for Zn^{2+} ions in ErZO films behaves as a donor providing an extra free electron, thus increasing the thin-film conductivity.[22,26,27,34,35] The experimental results demonstrate that Er-doped ZnO (ErZO) films exhibit good electrical properties and high transmittance, which is consistent with the above hypothesis. We also compared the application of ErZO and ITO anodes in OLEDs. The maximum current efficiency and power efficiency of the reference device (ITO) are 76.0 cd/A and 61.5 lm/W, respectively. Correspondingly, the maximum current efficiency and power efficiency of the ErZO based OLED device can reach 86.5 cd/A and 68.4 lm/W. It indicates that ErZO TCO thin films are good candidates for future optoelectronics applications.

Figure 1(a) shows the carrier concentration and mobility dependence on the Er composition of the ErZO films deposited on glass substrates (data also tabulated in Table I). The carrier concentration increases from 5×10^{19}/cm^3 to 5×10^{20}/cm^3 as the Er composition increases from 0.5 wt. % to 1.0 wt. % and does not change as the Er composition further increases to 2 wt. %. The electron concentrations of the 1.0 wt. % and 2.0 wt. % Er-doped samples are significantly higher than that of the undoped ZnO sample ($\sim 1 \times 10^{19}$/cm^3) fabricated by a similar PLD method, implying the donor effect of the Er-dopant.[34] Because of the large Er^{3+} radius, Er^{3+} is expected to occupy the relatively large Zn^{2+} site rather than the O^{2-} site in the ZnO lattice, which agrees with the x-ray absorption spectroscopy result that the first nearest neighbor atom of Er is O.[35] First principles calculation studies showed that Er_{Zn} has a 4f degenerate electron state above the conduction band minimum and contributes for the *n*-type conductivity.[26,27] The electron mobility remains roughly constant at ~28 cm^2/V·s for all the Er-doped ZnO samples with different Er compositions. The resistivity of the Er-doped ZnO samples with Er compositions of 0.5, 1, and 2 wt. % is 4.0×10^{-3}, 3.4×10^{-4}, and 4.9×10^{-4} Ω/cm, respectively.

Figure 2 shows the XRD spectra of the Er-doped samples with different Er-compositions of 0.5, 1, and 2 wt. %, which have peaks at around 34.5°, which correspond to the (002) diffraction peak of hexagonal wurtzite ZnO.[21] The absence of Er-oxide related diffraction peaks in the range indicates that there is no secondary phase of Er_2O_3 in the ErZO films. The *c*-axis lattice constant was calculated by the Bragg relation, and the average grain size was found by Scherrer's equation, whereas the results are listed in Table I. As the Er composition increases from 0.5 wt. % to 2 wt. %, the grain size decreases from ~28 nm to ~19 nm, while the c-axis lattice constant is around 5.19 Å.

The surface morphology and cross-sectional SEM images of ZnO and ErZO films were characterized by SEM. Figure 3 demonstrates the surface topography and thickness of ZnO, 0.5 wt. % ErZO, and 1.0 wt. % ErZO films, respectively. From the SEM images, these three

TABLE I. Structural, electrical, and optical properties of ErZO films with different Er concentrations.

Er content (wt. %)	*c*-Axis lattice constant (Å)	FWHM (002) (deg)	Grain size (nm)	Carrier concentration (/cm^3)	Mobility (cm$_2$/V·s)	Resistivity (Ω/cm)	Sheet resistivity (Ω/□)	Avg. transmittance (400–800 nm) (%)	Bandgap (eV)
0	5.192	0.30	26.78	1.45×10^{19}	21.7	1.99×10^{-2}	1370	90.5%	3.22
0.5	5.194	0.29	27.70	5.37×10^{19}	29.1	3.99×10^{-3}	266.2	89.0%	3.24
1	5.186	0.35	22.96	5.85×10^{20}	27.3	3.39×10^{-4}	26.07	93.3%	3.30
2	5.188	0.42	19.13	4.66×10^{20}	27.2	4.92×10^{-4}	32.80	90.3%	3.32

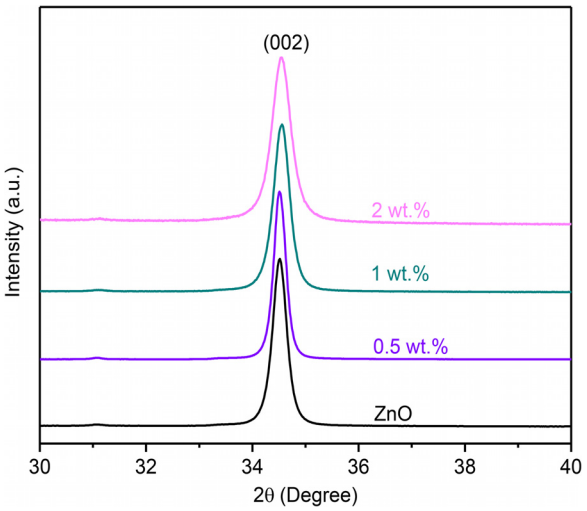

FIG. 2. XRD patterns for ZnO and 0.5–2 wt. % Er-doped ZnO films.

films exhibit good flatness and the crystal grain size is dependent on the Er concentration. The thickness of films is around 150 nm. Elemental dispersion spectroscopy (EDS) was also performed on these films, and the results are shown in Fig. S1. The EDS spectrum of each film shows the signals of Zn, O, Si, and Ca, where the signals of Si and Ga are only from the glass substrate. Because the Er concentration is too low, there is no signal for Er element due to the low doping content. The average crystal grain size of the 0.5 wt. % ErZO film is larger than those of the ZnO and 1.0 wt. % ErZO films, which is consistent with the narrow FWHM of the 0.5 wt. % ErZO film and wide FWHM of the 1.0 wt. % ErZO film. Therefore, the increase in the Er content brings about the smaller grain size and a relatively poor crystalline structure in the Er-doped ZnO sample due to the mismatch radius of Er^{3+} (0.89 Å) to the ZnO lattice (radius of Zn^{2+} is 0.74 Å).

The transmittance of the ErZO films with different Er contents (0.5–2 wt. %) and also the undoped ZnO film was characterized in the wavelength range of 350–900 nm. Figure 4(a) shows that the average transmittance of ErZO films is all above 85% in the range of 400–800 nm. Among them, 1 wt. % ErZO films exhibit the superior optical properties with the average transmittance of 93.3%. The inset of Fig. 4(a) shows the absorption spectra of ErZO films, which indicate that the bandgap of ErZO films increases slightly with the increasing Er composition. The blue-shift of the absorption edge is due to the Burstein-Moss effect as the Er-doped ZnO samples have the electron concentration as high as $\sim 10^{20}$ cm^{-3}.[23,24] The optical bandgaps of ErZO films are around 3.22–3.32 eV (Table I).

Room temperature PL spectra of the pure ZnO film and 1.0 wt. % ErZO film are shown in Fig. 4(b). Both the near band edge emission (NBE) and defect emission (DE) peaking at ~400 nm and ~500 nm are found in the two spectra, respectively. The DE with the peak at ~500 nm of ZnO is associated with intrinsic defects like Zn-vacancy

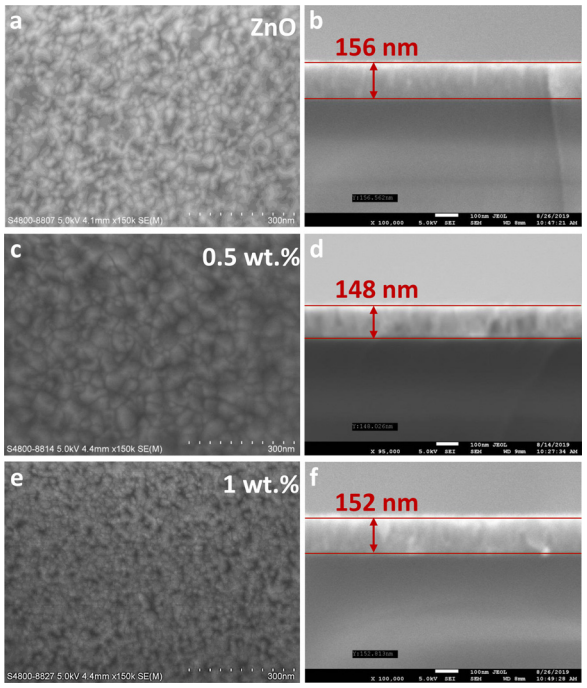

FIG. 3. SEM images and cross-sectional SEM images of (a) and (b) ZnO, (c) and (d) 0.5 wt. %, and (e) and (f) 1 wt. % Er-doped ZnO films.

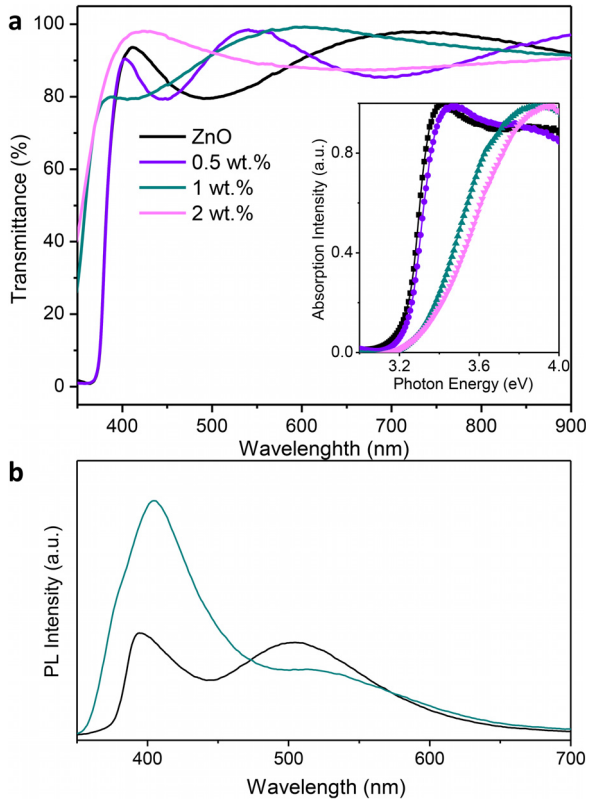

FIG. 4. (a) The optical transmittance of ErZO films with different doping concentrations (0–2 wt. %). Inset: the corresponding absorption spectra of ErZO films. (b) The photoluminescence (PL) spectra of the ZnO and 1 wt. % ErZO films at room temperature.

and O-vacancy.[25,28] The calculated values of I_{NBE}/I_{DE} for ZnO and ErZO films were 0.488 and 1.396, respectively. This indicated that the ErZO film had fewer defects than those in the ZnO film.[11]

A schematic diagram of the multilayered OLEDs is shown in Fig. 5(a), which consists of anode (ITO or ErZO), MoO_3 (molybdenum(VI) oxide), TAPC (di-[4-(N,N-di-p-tolyl-amino)-phenyl]cyclohexane), TcTa (4,4′,4″-tris(carbazol-9-yl)triphenylamine), CBP (4,4′-bis(carbazol-9-yl)biphenyl): $Ir(ppy)_2(acac)$ (bis(2-phenylpyridine)(acetylacetonato)iridium(III)), TPBi (1,3,5-tris(1-phenyl-1Hbenzimidazol-2-yl)benzene), Liq (8-hydroxyquinolinolato-lithium), and Al (aluminium). The electroluminescence (EL) intensity of the device based on ErZO is higher than that of the reference device with ITO as the anode at 1 mA/cm^2 [Fig. 5(b)]. Due to the difference in conductivity and work function between ITO and ErZO, the space charge density in the emission layer and the position of the carrier recombination zone are effectively adjusted, causing the variation of EL spectra of OLED devices.[31–33] In the device, the electrode has a large energy level difference with the highest occupied molecular orbital (HOMO) level of the organic material. Therefore, we add an electron injection layer of MoO_3 between the electrode and the organic layer to reduce the injection barrier. The work functions of ITO and ErZO are 4.5 and 4.3 eV;[29] and after evaporation of MoO_3, the corresponding work functions are changed to 5.0 and 4.5 eV (Fig. S2). Thus, the barrier from the electrode to the organic material is reduced. However, the work function of the two electrodes still has a difference of 0.5 eV, which results in the larger driving voltage required for holes from ErZO/MoO_3 to the organic layer than the driving voltage required for ITO/MoO_3 to the organic layer [Fig. 5(c)]. For example, when these OLED devices are driven at a current density of 0.2 mA/cm^2, the corresponding voltage of the device based on ErZO is 3.97 V, which is a little higher than that (3.88 V) of the reference device based on ITO. However, the power efficiency, current efficiency, and luminance of the ErZO based device are higher than those of the ITO based device [Fig. 5(d)]. When these

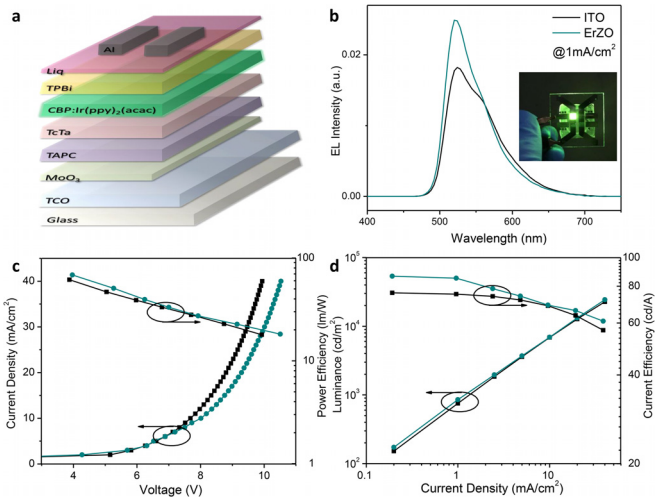

FIG. 5. (a) Schematic diagram of the device structure. (b) EL spectra of the ITO and ErZO based devices at 1 mA/cm^2. Inset: the image of the device (ErZO) driven at 10 mA/cm^2. (c) Current density-voltage-power efficiency and (d) luminance-current efficiency with current density for the ITO and ErZO based OLEDs.

OLED devices are driven at a current density of 0.2 mA/cm^2, the corresponding power efficiency and current efficiency of the ErZO based device are 68.4 lm/W and 86.5 cd/A, respectively, which are higher than that (61.5 lm/W and 76.0 cd/A) of the ITO based device. Moreover, when the current density is at 40 mA/cm^2, the maximum luminance of these OLED devices is 24 360 (ErZO) and 22 690 cd/m^2 (ITO). The detailed device performance of OLEDs is summarized in Table S1. The reflective index of ITO at 520 and 550 nm is 1.95 and 1.93, respectively.[30] The corresponding reflective index of ErZO we measured by ellipsometry is 1.70 and 1.74. The reflective index of organic material is around 1.75.[30] Thus, the ErZO electrode is more matched with organic material in terms of the reflective index, which could reduce the optical waveguide effect on the side of the transparent electrodes and improve the overall device performance. Furthermore, we test the lifetime of ITO and ErZO based devices at the drive current density of 10 mA/cm^2. As shown in Fig. S3, the half-lifetime (T_{50}) is almost the same (around 11 h). The EL spectra of ErZO based OLEDs measured at 0.2–40 mA/cm^2 exhibit the same emission shape. Therefore, the ErZO based OLEDs show good structural and EL stability. The attractive device performance confirms the functionality of ErZO films in OLED applications. Besides, we forecast that if the ErZO film is employed as the cathode in inverted optoelectronic devices, the overall device performance will be superior considering its high transmittance and matched energy level with organic transporting materials.

In summary, Er-doped ZnO TCO thin films on a glass substrate with various Er doping concentrations (0.5–2 wt. %) were fabricated by the PLD technique. The Er dopant substituted the Zn site and acted as a shallow donor in the crystal structure. The high electron concentration on the order of 10^{20}/cm^3 is attributed to the impurity of the Er element. Thin films with quite high optical transmittance (~93.3%) and a low resistivity of 3.39×10^{-4} Ω/cm can be obtained simultaneously, which widens the application of the as-grown Er-doped ZnO thin films. We have developed OLED devices by employing ErZO films as the anodes, respectively. The power efficiency and current efficiency of OLEDs with ErZO anodes are 68.4 lm/W and 86.5 cd/A, respectively, which are much higher than that (61.5 lm/W and 76.0 cd/A) of ITO references. Therefore, these mentioned beneficial characteristics and good EL performance confirm the future applications of ErZO thin films in the field of optoelectronics.

See the supplementary material for the experimental method, EDS spectra of ZnO and ErZO films, UPS spectra of ErZO, ITO/MoO_3, ErZO/MoO_3 films, the stability data for the OLED devices with ITO and ErZO as electrodes, and the summary of the device performance.

We would like to thank Mr. W. K. Ho for his professional guidance in the SEM measurement.

REFERENCES

[1]K. Badeker, Ann. Phys. **327**, 749 (1907).
[2]K. Nomura, H. Ohta, A. Takagi, T. Kamiya, M. Hirano, and H. Hosono, Nat. **432**, 488 (2004).
[3]S. S. Shin, E. J. Yeom, W. S. Yang, S. Hur, M. G. Kim, J. Im, J. Seo, J. H. Noh, and S. Seok, Sci. **356**, 167 (2017).
[4]J. Cui, A. Wang, N. L. Edleman, J. Ni, P. Lee, N. R. Armstrong, and T. J. Marks, Adv. Mater. **13**, 1476 (2001).

[5]X. L. Chen, W. R. Guo, L. M. Xie, C. T. Wei, J. Y. Zhuang, W. M. Su, and Z. Cui, ACS Appl. Mater. Interfaces **9**, 37048 (2017).
[6]L. Schmidt-Mende and J. L. MacManus-Driscoll, Mater. Today **10**(5), 40 (2007).
[7]S. Heo, S. K. Sharma, S. Lee, Y. Lee, C. Kim, B. Lee, H. Lee, and D. Y. Kim, Thin Solid Films **558**, 27 (2014).
[8]J. Brunckoa, P. Šuttab, M. Netrvalováb, M. Michalkaa, and A. Vincze, Vacuum **159**, 134 (2019).
[9]T. Coman, D. Timpu, V. Nica, C. Vitelaru, A. P. Rambu, G. Stoian, M. Olaru, and C. Ursu, Appl. Surf. Sci. **418**, 456 (2017).
[10]C. M. Pak, S. C. Su, C. C. Ling, Y. M. Lu, and D. L. Zhu, J. Phys. D **46**, 135104 (2013).
[11]Y. J. Choi and H. H. Park, J. Mater. Chem. C **2**, 98 (2014).
[12]Y. Yang, Y. P. Li, C. X. Wang, C. Zhu, C. Y. Lv, X. Y. Ma, and D. R. Yang, Adv. Opt. Mater. **2**, 240 (2014).
[13]M. Balestrieri, M. Gallart, M. Ziegler, P. Bazylewski, G. Ferblantier, G. Schmerber, G. S. Chang, P. Gilliot, D. Muller, A. Slaoui, S. Colis, and A. Dinia, J. Phys. Chem. C **118**, 13775 (2014).
[14]V. Kumar, O. M. Ntwaeaborwa, T. Soga, V. Dutta, and H. C. Swart, ACS Photonics **4**, 2613 (2017).
[15]E. F. Pecora, T. I. Murphy, and L. D. Negro, Appl. Phys. Lett. **101**, 191115 (2012).
[16]T. Minami, T. Yamamoto, and T. Miyata, Thin Solid Films **366**, 63 (2000).
[17]J. S. Luo, J. Lin, N. Zhang, X. Y. Guo, L. G. Zhang, Y. S. Hu, Y. Lv, Y. F. Zhu, and X. Y. Liu, J. Mater. Chem. C **6**, 5542 (2018).
[18]N. Babayevska, B. Peplińska, M. Jarek, L. Yate, K. Tadyszak, J. Gapiński, I. Iatsunskyia, and S. Jurga, RSC Adv. **6**, 89305 (2016).
[19]A. Azarov, A. Galeckas, A. Hallen, A. Kuznetsov, E. Monakhov, and B. G. Svensson, J. Appl. Phys. **118**, 125703 (2015).
[20]F. Azad, C. Luo, S. Su, M. Younas, W. Azeem, A. Kuznetsov, A. Azarov, K. Shih, C. Liao, A. Maqsood, and F. C. C. Ling, J. Appl. Phys. **121**, 235701 (2017).
[21]A. Wolcott, W. A. Smith, T. R. Kuykendall, Y. P. Zhao, and J. Z. Zhang, Adv. Funct. Mater. **19**, 1849 (2009).
[22]M. Khalid, M. Ziese, A. Setzer, P. Esquinazi, M. Lorenz, H. Hochmuth, M. Grundmann, D. Spemann, T. Butz, G. Brauer, W. Anwand, G. Fischer, W. A. Adeagbo, W. Hergert, and A. Erns, Phys. Rev. B **80**, 035331 (2009).
[23]H. Yoshimura, G. E. W. Bauer, and H. Sakaki, Phys. Rev. B **38**, 10791 (1988).
[24]Y. Q. Wang, W. Tang, J. Liu, and L. Zhang, Appl. Phys. Lett. **106**, 162101 (2015).
[25]Z. L. Wang, S. C. Su, M. Younas, F. C. C. Ling, W. Anwand, and A. Wagner, RSC Adv. **5**, 12530 (2015).
[26]S. J. Wang, X. B. Shi, and J. M. Li, RSC Adv. **6**, 107865 (2016).
[27]H. L. Li, Y. B. Lv, J. Z. Li, and K. Yu, J. Alloys Compd. **617**, 102 (2014).
[28]C. Ton-That, L. Weston, and M. R. Phillips, Phys. Rev. B **86**, 115205 (2012).
[29]Y. Park, V. Choong, and Y. Gao, Appl. Phys. Lett. **68**, 2699 (1996).
[30]R. J. Moerland and J. P. Hoogenboom, Optica **3**, 112 (2016).
[31]Y. C. Zhou, J. Zhou, J. M. Zhao, S. T. Zhang, Y. Q. Zhan, X. Z. Wang, Y. Wu, X. M. Ding, X. M. Ding, and X. Y. Hou, Appl. Phys. A **83**, 465 (2006).
[32]Y. X. Wu, L. D. Wang, G. T. Lei, and Y. Qiu, J. Appl. Phys. **97**, 103105 (2005).
[33]J. Xiao, H. Zhu, X. X. Wang, X. Gao, Z. H. Yang, X. H. Zhang, and S. D. Wang, J. Appl. Phys. **112**, 014513 (2012).
[34]A. K. Pradhan, L. Douglas, H. Mustafa, R. Mundle, D. Hunter, and C. E. Bonner, Appl. Phys. Lett. **90**, 072108 (2007).
[35]M. Ishii, S. Komuro, T. Morikawa, and Y. Aoyagi, J. Appl. Phys. **89**, 3679 (2001).